INTERMOLECULAR POTENTIALS FOR α-GLYCINE FROM RAMAN AND INFRARED SCATTERING MEASUREMENTS

B. ANDREWS AND B. H. TORRIE
Guelph-Waterloo Program for Graduate Work in Physics, Waterloo Campus, University of Waterloo, Waterloo, Ontario, Canada N2L 3G1

B. M. POWELL
Atomic Energy of Canada Limited, Chalk River Nuclear Laboratories, Chalk River, Ontario, KOJ 1JO Canada

ABSTRACT The frequencies of intermolecular modes in α-glycine-d_0 and -d_5 have been measured at 300 and 85 K by Raman and infrared scattering techniques. These frequencies were analyzed in terms of simple analytic interatomic potentials. Buckingham potentials were assumed for the nonbonded and hydrogen-bond interactions, and Coulomb and screened Coulomb potentials were assumed for the electrostatic interactions. The observed frequencies are well described by the simple model and the parameters of the hydrogen-bond potentials and the molecular charge distribution were determined from the analysis.

INTRODUCTION

The conformations and functions of biological macromolecules are determined by their interatomic and intermolecular interactions. The size and complexity of these macromolecules make a realistic calculation of such interactions difficult, if not impossible, at present. A possible alternative approach is to study the smaller constituent molecules of which the macromolecules are composed and to assume the interactions derived from these studies are transferable to the macromolecules themselves. The principal constituents of protein are amino acids, the simplest of which is glycine. We may hope that study of the interaction potentials in glycine will provide some information about the corresponding interactions in protein.

Crystalline glycine ($H_3N^+ \cdot CH_2 \cdot COO^-$) exists in three phases, with the α-phase being stable at room temperature and below. The structure of α-glycine is monoclinic (space group $P2_1/n$) with four molecules in the unit cell (1–3). The molecules are hydrogen bonded in layers perpendicular to the *b*-axis and the layers themselves are hydrogen bonded in pairs to form antiparallel double layers. Raman scattering measurements have been made for α-glycine-d_0 (4, 5) and for α-glycine-d_0 -N-d_3, -C-d_2 and -d_5 (6, 7). All these measurements were made at room temperature. Infrared measurements have also been made for α-glycine-d_0 and -N-d_3 at room temperature (7, 8) and for α-glycine-d_0 at 113 K (8). Interatomic potentials have been developed to interpret both Raman (5, 6) and infrared results (7), while the lattice energy and packing configuration were also calculated from empirical interatomic potential functions (9). Inelastic neutron scattering measurements (10) of intermolecular mode dispersion relations were recently made for α-glycine-d_5.

In the present paper we report new Raman scattering measurements of the intermolecular mode frequencies at the zone-center in α-glycine-d_5 and -d_0 at room temperature and at 85 K and infrared measurements on -d_5 at room temperature and at 98 K. The room temperature data for -d_5 together with the *ungerade* frequency measured by neutron scattering are successfully interpreted in terms of a set of simple interatomic potentials. The nonbonded and the hydrogen-bond interactions are represented by Buckingham potentials and the electrostatic interactions are represented by simple Coulomb and screened Coulomb potentials. The molecular charge distribution and the parameters of the hydrogen-bond potentials are derived from the analysis. Preliminary results of the experiment have been reported previously (11).

EXPERIMENTAL DETAILS AND RESULTS

The deuterated glycine (98% deuteration) was supplied by Merck, Sharp and Dohme Canada Ltd., Montreal. Single crystals of α-glycine were grown by slow evaporation of aqueous solutions of glycine-d_5 in D_2O and of -d_0 in H_2O.

The Raman spectra of several crystals were measured with the 514.5-nm line of a 165 argon ion laser (Spectra-Physics, Inc., San Jose, CA) operating at 0.4 W. The light scattered at 90° was dispersed in a double monochromator (model 1401; Spex Industries, Inc., Edison, NJ) and detected with a cooled photomultiplier (model C31034; RCA Corp., New York, NY). A photon counting system with output to a Nova 2 computer (Data General Corp., Westboro, MA) was used to process, store and display the spectra. Measurements at low temperature were made in a glass cryostat with the sample clamped to a cold finger. Typical spectra for α-glycine-d_0 and -d_5 are shown in Figs. 1 and 2, respectively.

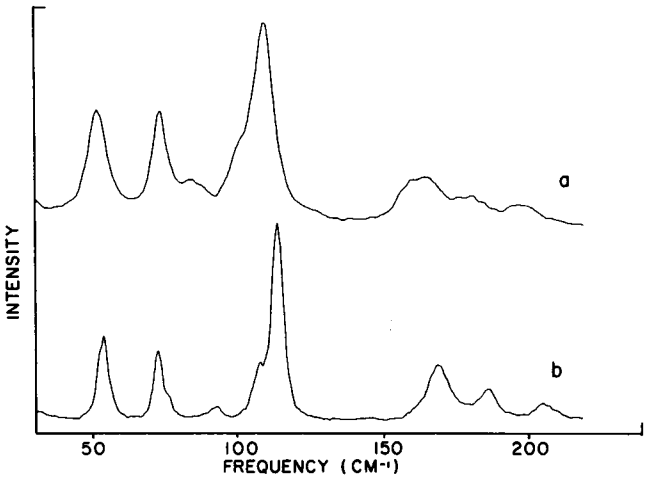

FIGURE 1 Experimental Raman spectra of α-glycine-d_0. (*a*) T = 300 K; (*b*) T = 85 K.

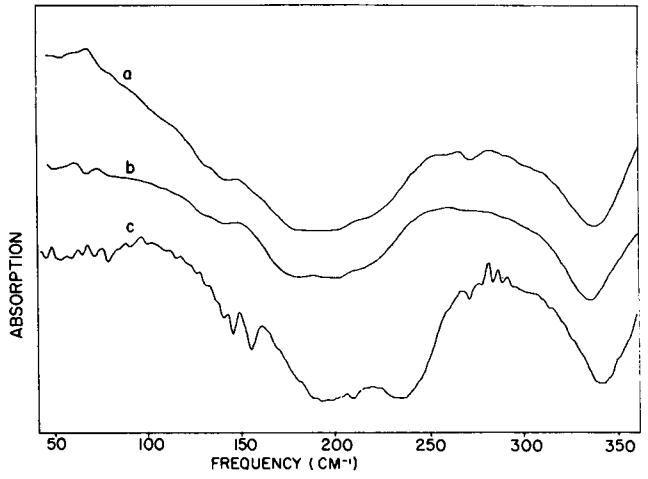

FIGURE 3 Experimental infrared spectra of α-glycine-d_5. (*a*) Powder at T = 300 K; (*b*) Nujol mull at T = 300 K;, (*c*) powder at T = 98 K.

The infrared spectra were recorded with a R11C-Beckman 620 Fourier spectrophotometer (Beckman Instruments Inc., Fulton, CA) connected to the Nova 2 computer. Several single crystals were ground to a fine powder and smeared on a polyethylene backing plate in either pure form or mixed with Nujol mull. The two types of samples produced similar spectra for glycine-d_5, but for glycine-d_0 only the Nujol mull gave spectra that matched those of reference 8. The pure sample produced a broad absorption band with no fine structure. Low temperature spectra were obtained using a conventional glass cryostat with liquid nitrogen. Spectra for glycine-d_5 are shown in Fig. 3.

A factor group analysis shows that there are 12 Raman active and 9 infrared active intermolecular modes with nonzero frequencies. The symmetry representations are $6A_g + 6B_g$ and $5A_u + 4B_u$ for the Raman and infrared active modes, respectively. Good polarization data could not be obtained in our Raman measurements. This is probably due to poor quality single crystal specimens. Other authors have claimed more success in identifying A_g and B_g modes with polarized Raman measurements. However, the symmetry assignments of different authors are inconsistent and several reported frequencies are common to both symmetry representations. Our results are given in Tables IA and B, where they are compared with those of previous measurements. The errors given in the table are derived from four to six separate Raman spectra. They show the range of frequencies found by a peak finding program. As would be expected, the magnitude of the errors depends strongly on the experimental width of the corresponding peak. It can be seen from Table IA that at 300 K the various sets of frequencies are in fair agreement with each other. However, weak Raman lines at 151 cm^{-1} (for -d_5) and 155 cm^{-1} (for -d_0) were reported by Machida et al. (6) and Castellucci et al. (5); the latter authors interpret the higher external frequencies for all symmetry representations to be much higher than those of other authors. The comparison of the spectra at 300 and 85 K in Figs. 1 and 2 shows that all peaks are significantly sharper at the lower temperature and some of the broader peaks are split at 85 K. As a result, several more Raman frequencies were observed at 85 K, particularly for glycine -d_5. In total we observed 8 Raman frequencies for glycine -d_0 and 10 Raman frequencies for glycine -d_5, rather than the 12 possible frequencies.

Our infrared results are also given in Table IB and compared with those of other authors. The infrared results at 300 K for glycine -d_5 indicate three frequencies that would be expected to correspond to the frequencies derived for glycine -d_0 by Feairheller and Miller (8). However, our frequencies are all higher than the corresponding ones of Feairheller and Miller. This is contrary to the observed effects of deuteration on the Raman frequencies. Our results at 98 K for -d_5 show a similar effect when

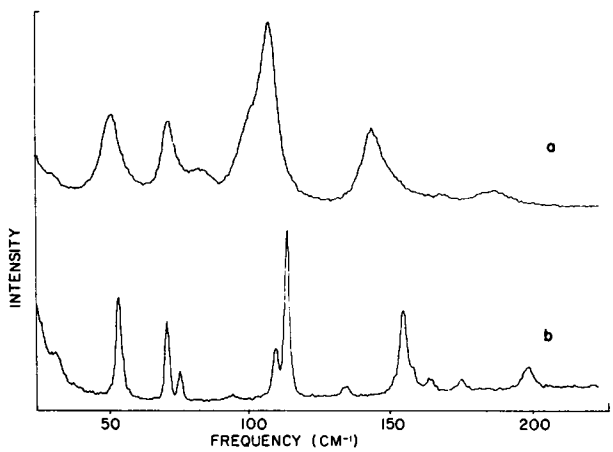

FIGURE 2 Experimental Raman spectra of α-glycine-d_5. (*a*) T = 300 K; (*b*) T = 85 K.

TABLE IA
EXPERIMENTAL INTERMOLECULAR MODE FREQUENCIES IN α-GLYCINE (GLYCINE-d_0)*

Raman spectroscopy					Infrared spectroscopy		
		References for data					
This work		6	4	5	7	8	
85 K			300 K				13 K
187 ± 2	180 ± 2	178	180	181(B_g)	175	170	189
170 ± 2	164 ± 3	163(B_g)	164	164(B_g)	140	138	144
		155(A_g)		156(A_g)		132	140
116 ± 1	109.9 ± 0.5	109	110	109	91	—	—
109 ± 1	—	—	—	—	—	—	—
94 ± 2	86 ± 2	84(B_g)	85	—	—	—	—
78 ± 1	—	—	—	—	—	—	—
74 ± 1	74.5 ± 0.5	74	74	73(B_g)	—	—	—
55 ± 1	52.7 ± 0.5	51	52	52(A_g)	—	—	—

*In units of reciprocal centimeters (cm^{-1}).

TABLE 1B
EXPERIMENTAL INTERMOLECULAR MODE FREQUENCIES IN α-GLYCINE (GLYCINE-d_5)*

Raman spectroscopy			Infrared spectroscopy	
References for data				
This work		6	This work	
85K		300K		98K
176.3 ± 0.7	164 ± 2	168(B_g)	180	193
	—	167(A_g)	143	155
158.5 ± 0.5	—	151(A_g)	131	146
	—	—	—	141
154.5 ± 0.5	144.6 ± 0.8	144(B_g)	—	—
138.8 ± 0.8	—	—	—	—
114.7 ± 0.7	107.8 ± 0.5	107	—	—
110.3 ± 0.7	—	—	—	—
95.4 ± 0.6	83 ± 2	84(B_g)	—	—
76.6 ± 0.6	—	—	—	—
72.1 ± 0.4	72.4 ± 0.8	72	—	—
55.1 ± 0.4	52.0 ± 0.5	51	—	—

*In units of reciprocal centimeters (cm^{-1}).

compared with the data of Feairheller and Miller on -d_0 at 113 K. However, we also observe an additional frequency at 155 cm^{-1}. Consequently, at 98 K, we have observed four of the nine possible infrared active modes.

ANALYSIS

We have analyzed our results in terms of analytic interatomic potentials in an attempt to derive a simple potential for the N—H···O hydrogen bonds and to derive an experimental molecular charge distribution for α-glycine. The analysis is analogous to that carried out by Powell and Martel (12) for DNA base complexes. We describe all nonbonded interactions by Buckingham pair potentials of the form:

$$v(r_{ij}) = -\frac{A_{ij}}{r_{ij}^6} + B_{ij}\exp(-C_{ij}r_{ij}), \qquad (1)$$

where r_{ij} is the interatomic separation of atoms i and j and A_{ij}, B_{ij}, C_{ij} are the constants of the potential for atom species i, j. We assume the glycine molecules are rigid and represent the hydrogen bonds X—H···Y by Buckingham potentials between atoms H and Y. Following Jönsson and Kvick (3) we consider the three shortest intermolecular H···O bonds to have the character of hydrogen bonds, i.e., N—H(1)···O(1), N—H(2)···O(2), and N—H(3)···O(2) and assume them to have the same potential function. We follow Schroeder and Lippincott (13) in treating the nonlinearity of these hydrogen bonds by using, as the separation r_{ij}, the projection of the H···Y distance on to the line X—Y. The effect of this nonlinearity is only ≈1% for the H···O separation for the N—H(3)···O(2) bond and is even smaller for the other two hydrogen bonds. The molecular charge distribution is represented by point charges located at the atomic positions. For charges on the atoms in the hydrogen bonds the interaction is assumed to have a simple Coulomb form. For charges on atoms in the nonbonded interactions, the potentials are assumed to have a screened Coulomb form

$$v(r_{ij}) = \frac{Z_iZ_j}{r_{ij}}\exp(-Kr_{ij}),$$

where Z_i, Z_j are the charges on atoms i, j, respectively and K, is an inverse screening length, assumed to be identical for all atom pairs, i, j.

The values for the parameters of the nonbonded interactions are those used by Powell and Martel (12) in their calculations for DNA base complexes. The parameters for the interactions that do not involve hydrogen are listed in Table II. Initial values for the nonbonded interactions involving hydrogen were also taken from Powell and Martel, while the hydrogen bond parameters were those found for the N—H···O bond in cytosine monohydrate by the same authors. The initial molecular charge distribution was that calculated by Momany et al. (9) and the inverse screening length, K, was fixed at 0.333 $Å^{-1}$. This value was chosen because the atomic and molecular packing (1, 2) shows that the closest molecular contacts, both within and between layers, are ≈3 Å. The summation ranges were 6 and 11 Å for the nonbonded and Coulomb interactions, respectively. Test calculations showed that the frequency of the lowest A_u mode was the only one significantly affected by increasing either of these ranges.

Since it is experimentally difficult to distinguish between A_g and B_g modes, the six most intense peaks in the Raman spectrum of α-glycine-d_5 at 300 K were assumed to be A_g modes. This assumption does not cause a large error, for preliminary calculations showed that the frequencies of corresponding A_g and B_g modes differed by <10%. The same calculations also showed that the lowest A_u mode had a significantly lower frequency than those of all other intermolecular modes at Γ. Consequently, this mode was interpreted as the low-lying *ungerade* mode observed by inelastic neutron scattering (10). Its frequency, together with the six experimental Raman frequencies, comprised the data in terms of which the model parameters were adjusted. The net molecular charge was fixed at zero, the

TABLE II
PARAMETERS SPECIFYING THE NONBONDED BUCKINGHAM POTENTIALS

Atom pair	A	B	C
	$kcal \cdot Å^6 \cdot mol^{-1}$	$kcal \cdot mol^{-1}$	cm^{-1}
C—C	358	42,000	3.58
C—N	308	42,640	3.68
C—O	313	57,100	3.85
N—N	259	42,000	3.78
N—O	256	57,200	3.98
O—O	259	77,000	4.18

methylene group was maintained neutral, the charges on the three amine hydrogens were kept equal, and the charges on O(1) and O(2) were held equal to each other. The parameters of the nonbonded interactions and the parameter C of the hydrogen bond were kept fixed. The adjustable parameters were thus A and B for the hydrogen bond potential and the charges on the N, C(1), C(2) and O(1) atoms. However, the parameters of the nonbonded interactions involving hydrogen were also found to affect the minimization, and some adjustment of these parameters was also made. The quantity minimized, S^2, is defined as:

$$S^2 = \sum_i \frac{[\nu_i(\text{obs}) - \nu_i(\text{calc})]^2}{(\Delta\nu_i)^2},$$

where ν_i(obs) and ν_i(calc) are the observed and calculated frequencies, respectively, $\Delta\nu_i$ is the experimental error in ν_i (obs), and the summation is over the A_u and the six A_g modes. The optimum values of the adjustable parameters are given in Table III and the Buckingham potential for the N—H...O bond is shown in Fig. 4. The comparison between the observed and calculated frequencies for both the α-glycine -d_5 and -d_0 at 300 K is shown in Table IV.

DISCUSSION

It is clear this simple model gives a reasonable description of the observed intermolecular mode frequencies in α-glycine-d_5. Both the frequency of the A_u mode and the over-all bandwidth of the A_g modes are well reproduced. The largest discrepancy ($\approx$11 cm^{-1}) occurs for the second highest frequency A_g mode, whereas the mean discrepancy for the A_g modes is $\approx$7 cm^{-1}. This compares with a mean discrepancy of 8.2 cm^{-1} for the 5 A_g modes and 10 cm^{-1} for the 11 A_g and B_g modes observed and calculated by Machida et al. (6). The model proposed by Castellucci et al. (5) was fitted to their Raman data. This data included several modes with frequencies significantly higher than any identified as intermolecular in either the present paper

TABLE III
VALUES OF ADJUSTABLE PARAMETERS IN THE MINIMIZATION

		A	B	C
Hydrogen bond				
N—H · · · O		228	43,000	5.14
Atom pair				
C—H		214	30,000	4.12
N—H		121	24,000	4.25
O—H		188	25,000	4.50
H—H		89	34,000	4.86
Atom	C1	C2	N	O
Charge*	0.645	0.000	−0.022	−0.475

The parameters A, B, and C have the units specified in Table II.
*In unit of $|e|$ for the electron charge.

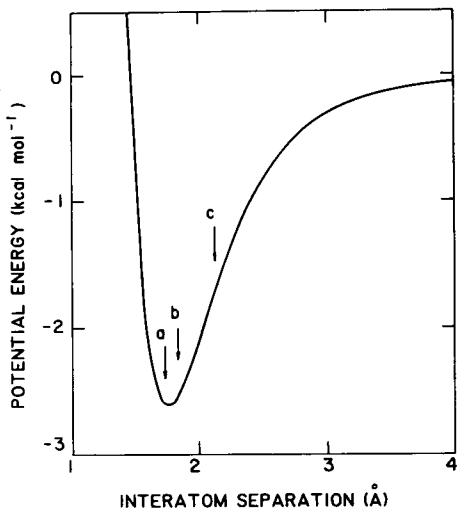

FIGURE 4 Calculated Buckingham potential for N—H···O hydrogen bonds in α-glycine. The arrows a, b, c show the H···O separation for the N—H(1)···O(1), N—H(2)···O(2), N—H(3)···O(2) bonds, respectively.

or by Machida et al. A direct comparison of the present model with that of Castellucci et al. is thus not meaningful, especially since their model does not predict the low frequency A_u mode observed by Powell and Martel (10). The induced dipole moments calculated for the *ungerade* modes by the present model are shown in Table V. In view of the rather sparse experimental data, a comparison between the observed infrared intensities and these calcu-

TABLE IV
COMPARISON OF THE OBSERVED AND CALCULATED FREQUENCIES IN α-GLYCINE-d_0 AND α-GLYCINE-d_5*

Mode	α-Glycine-d_0		α-Glycine-d_5	
	Observed	Calculated	Observed	Calculated
A_g	52.7	45	52	45
	74.5	68	72.4	67
	86	91	111	92
	109.9	111	107.8	110
	164	130	144.6	133
	180	176	164	175
B_g	—	48	—	47
	—	77	—	77
	—	83	—	83
	—	110	—	110
	—	122	—	124
	—	174	—	172
A_u	16	18	—	18
	—	43	—	43
	—	69	—	69
	—	117	—	117
	—	180	—	180
B_u	—	62	—	60
	—	91	—	94
	—	125	—	125
	—	180	—	180

*In units of reciprocal centimeters (cm^{-1}).

TABLE V
CALCULATED INDUCED DIPOLE MOMENTS FOR THE UNGERADE MODES IN α-GLYCINE-d_5

Mode	Calculated frequency	Induced dipole moment
	cm^{-1}	
A_u	18	0.91
	43	2.40
	69	0.53
	117	1.50
	180	0.14
B_u	60	0.11
	94	0.21
	125	1.00
	180	2.64

Units are arbitrary.

lated dipole moments is not very useful. The lowest A_u mode frequency agrees well with that observed by Powell and Martel (10). However, their suggestion that another low-lying *ungerade* mode exists at ≈33 cm^{-1} is only qualitatively correct. The next lowest *ungerade* mode is calculated to be an A_u mode at 43 cm^{-1}. Note that only two modes are calculated to occur with the same frequency and these belong to different symmetry representations. This is in contrast to the assignments of some authors, (4–8) for which several modes of different symmetries have common frequencies.

The calculated potential energy of a molecule is −46.6 kcal·mol^{-1}, corresponding to a sublimation energy of ≈25 kcal·mol^{-1}, in fair agreement with the measured sublimation energy of 32.7 kcal·mol^{-1} (14). The dominant contribution to the potential energy (≈59%) is from the electrostatic term in the hydrogen-bond interactions. The nonbonded interactions contribute a further 34% of the total, while the attractive potential from the Buckingham term in the hydrogen-bond interaction is partly cancelled by a repulsive potential from the Coulomb terms of the nonbonded interactions. The molecular charge distribution derived in the present analysis differs from all the calculated distributions (6, 9, 15) in having a large partial charge on C(1) whereas C(2) has zero partial charge. The overall charge distribution is more like those of Machida et al. (6) and Derissen et al. (15) than that of Momany et al. (9). The static molecular dipole moment is found from our charge distribution to be 8.71 (Debye) and has the largest component along the *c*-axis. This may be compared with experimental values of 13.1 D and 13.4 D obtained from measurements on aqueous solutions of glycine (16).

The assumption of "rigid molecules" is not well satisfied for α-glycine. The optical measurements of Machida et al. (7) show that the gap between the lowest intramolecular and highest intermolecular frequencies at Γ is only ≈17 cm^{-1}. The effect of including the interaction between these modes will be to lower the calculated value for the highest intermolecular mode. This would improve the agreement between the present calculation and the experimental frequency of this mode. The representation of the electrostatic components of the nonbonded interactions as a screened Coulomb potential is also clearly oversimplified. It views the molecules as charge distributions in a dielectric medium and considers only the lowest order interaction. But the introduction of some form of screening function or cut-off for the electrostatic interaction at large intermolecular separations seems physically reasonable. Greenberg et al. (17) introduced a step function description in their formulation of the molecular dielectric function to achieve this effect. The lowest A_u frequency depends on the value chosen for the inverse screening length and this length could be used as an adjustable parameter. A dielectric constant, $\epsilon \neq 1$, might also be included as a further parameter (17). However, these additional parameters, together with any arising from a more complex description of either the nonbonded or electrostatic interactions, can only be determined if more experimental data are available. An unambiguous identification of A_g and B_g frequencies would be helpful, together with measurements of more *ungerade* frequencies. Several of the zone boundary frequencies measured by inelastic neutron scattering should also be included in any further refinement and calculations are planned using this approach.

Received for publication 22 June 1982 and in final form 13 August 1982.

REFERENCES

1. Albrecht, G., and R. B. Corey. 1939. The crystal structure of glycine. *J. Am. Chem. Soc.* 61:1087–1103.
2. Marsh, R. E. 1958. A refinement of the crystal structure of glycine. *Acta Crystallogr.* 11:654–663.
3. Jönsson, P.-G., and A. Kvick. 1972. Precision neutron diffraction structure determination of protein and nucleic acid components. III. The crystal and molecular structure of the amino acid α-glycine. *Acta Crystallogr. Sect. B. Struct. Crystallogr. Cryst. Chem. 28:1827–1833.*
4. Stenbäch, H. 1976. On the Raman spectra of solid natural α-glycine and solid ^{15}N-substituted α-glycine. *J. Raman Spectrosc.* 5:49–55.
5. Castellucci, E., N. Neto, and S. Sbrana. 1976. Raman study and frequency calculation of glycine. *In* Proceedings of the 5th International Conference on Raman Spectroscopy. E. D. Schmid, J. Brandmueller and W. Kiefer, editors. Verlag, Freiburg. 550–551.
6. Machida, K., A. Kagayama, and Y. Saito. 1979. Polarised Raman spectra and intermolecular potential of α-glycine-C-d_2 and DL-alanine-α, β-d_4 crystals. *J. Raman Spectrosc.* 8:133–138.
7. Machido, K., A. Kagayama, Y. Saito, Y. Kuroda, and T. Uno. 1977. Vibration spectra and intermolecular potential of the α-form crystal of glycine. *Spectrochim. Acta. Part A. Mol. Spectrosc. 33:569–574.*
8. Feairheller, W., and J. T. Miller, Jr. 1971. The infrared spectra of amino acids and some simple polypeptides to 33 cm^{-1} at room and liquid nitrogen temperatures. *Appl. Spectrosc.* 25:175–182.
9. Momany, F., L. M. Carruthers, and H. A. Scheraga. 1974. Intermolecular potentials from crystal data. IV. Application of empirical potentials to the packing configurations and lattice energies in crystals of amino acids. *J. Phys. Chem.* 78:1621–1630.

10. Powell, B. M., and P. Martel. 1979. Low frequency intermolecular modes in deuterated α-glycine. *Chem. Phys. Lett.* 67:165–167.
11. Andrews, B., B. H. Torrie, and B. M. Powell. 1980. Lattice modes of deuterated α-glycine. *In* Proceedings of the 7th International Conference on Raman Spectroscopy. W. F. Murphy, editor. North Holland Publishing Co., New York. 110–111.
12. Powell, B. M., and P. Martel. 1981. Hydrogen bonding in DNA base complexes. *Biophys. J.* 34:311–323.
13. Schroeder, R., and E. R. Lippincott. 1957. Potential function model of hydrogen bonds. II. *J. Phys. Chem.* 61:921–928.
14. de Kruif, C. G., J. Voogd, and J. C. A. Offringa. 1979. Enthalpies of sublimation and vapour pressures of 14 amino acids and peptides. *J. Chem. Thermodynamics.* 11:651–656.
15. Derissen, J. T., P. H. Smit, and J. Voogd. 1977. On the calculation of the electrostatic lattice energies of α-, β-, and γ-glycine. *J. Phys. Chem.* 81:1474–1476.
16. Edward, J. T., P. G. Farrell, and J. L. Job. 1973. The dipole moments of 4-aminobicyclo [2.2.2] octane-1-carboxylic acid and some α, ω amino acids. *J. Phys. Chem.* 77:2191–2195.
17. Greenberg, D. A., C. D. Barry and G. R. Marshall. 1978. Investigation and parametrization of a molecular dielectric function. *J. Am. Chem. Soc.* 100:4020–4026.